

- (3) Jacrot, B. *Rep. Progr. Phys.* 1976, 39, 911.
 (4) Allen, M. P.; Tildesley, D. J. *Computer Simulation of Liquids*; Clarendon Press: Oxford, 1987.
 (5) McGreevy, R. L.; Pusztai, L. *Mol. Simul.* 1988, 1, 369.
 (6) McGreevy, R. L.; Pusztai, L. *Proc. R. Soc. London* 1990, 430, 241.
 (7) Ottewill, R. H. *Progr. Colloid Polym. Sci.* 1980, 67, 71.
 (8) McGreevy, R. L.; Howe, M. A.; Keen, D. A.; Clausen, K. N. *IOP Conf. Ser.* 1990, 107, 165.
 (9) Pusztai, L.; Tóth, G. *J. Chem. Phys.* 1991, 94, 3042.
 (10) McGreevy, R. L.; Howe, M. A. *Phys. Chem. Liq.* 1991, 24, 1.
 (11) Tóth, G.; Pusztai, L. *Chem. Phys.* 1992, 160, 405.
 (12) Pusztai, L. *Z. Naturforsch.* 1991, 46a, 69.

An EXAFS Study of the Metallofullerene YC_{82} : Is the Yttrium Inside the Cage?

L. Soderholm,* P. Wurz, K. R. Lykke, D. H. Parker,†

Argonne National Laboratory, Argonne, Illinois 60439

and F. W. Lytle

The Boeing Company, Seattle, Washington 98124 (Received: May 12, 1992; In Final Form: July 18, 1992)

A sample, determined by time-of-flight mass spectroscopy (TOFMS) to consist of YC_{82} as the major metal-fullerene complex, was analyzed by X-ray absorption spectroscopy. The Y is found to have 7 ± 1 near-neighbor C atoms at $2.35 \pm 0.02 \text{ \AA}$ and an Y neighbor at $4.05 \pm 0.05 \text{ \AA}$. The unequivocal observation of an Y-Y interaction is unexpected, since the mass spectral data show no indication of Y_2C_n as a major component of the sample. We believe that the combined TOFMS and extended X-ray absorption fine structure (EXAFS) results are not consistent with models that place the metal ion inside the fullerene cage. Instead, we propose that our data can be explained with a dimer of the form $C_{82}Y-X-YC_{82}$, where $-X-$ is a bridging carbon or oxygen species. The short Y-C near-neighbor distance indicates a strong, bonding interaction between the metal ion and the fullerene cage.

Introduction

It has been suggested that the cavity created inside the "soccerball-like" structure of the C_n fullerene clusters could trap metal ions to form endohedral complexes with interesting electron properties. Evidence for the formation of LaC_{60} , made by laser vaporization of a low-density graphite source impregnated with $LaCl_3$, was obtained by time-of-flight mass spectroscopy (TOFMS).¹ TOF peaks attributable to LaC_{60} or LaC_n^+ were identified, where n ranged from 44 to greater than 76. There was no evidence of clusters associated with more than one La ion; therefore, it was inferred that there is only one uniquely-stable binding site per C_n and that this site is inside the C_n cage. Photodissociation of metal-carbon clusters involves the successive loss of C_2 fragments, in a pattern similar to that obtained from photodissociation of the bare clusters.² The loss of C_2 rather than M^+ has been used to argue that the metal ion is sterically trapped inside the fullerene cage. This suggestion gains further support from the apparent stability of these metal complexes to reaction with either oxygen or moist air.³ In particular, LaC_{82} is found to be the only lanthanum fullerene to be produced by standard carbon-arc techniques that expose the soot to air.

A comparable stability of LaC_{82} and the bare cluster C_{84} has led to the description of the complex in terms of a La^{2+} ion inside a C_{82}^{2-} cage.³ This description has been shown to be inconsistent with EPR⁴ and XPS⁵ data, both of which indicate that La is nearly trivalent. The latter interpretation is more consistent with the known chemical stability of trivalent La, but the C_{82}^{3-} counterion is difficult to reconcile with the known stabilities of the bare clusters.

Recently, the unique stability of the single-metal-ion clusters has been brought into question by the discovery of a series of complexes La_nC_{84-2n} ($n = 0, 1, 2$), with La_2C_{80} as a major, extractable species from a La_2O_3 -loaded carbon-arc experiment.⁶ It has been suggested that the metal atom is incorporated into the cage framework itself, each La ion replacing two carbon atoms, rather than being trapped inside the cage structure.⁶

Recently, yttrium (Y) has been reported to be incorporated into the fullerene cages with even greater facility than La.⁵ The metallofullerenes YC_{60} and Y_2C_n are reported, with Y_2C_{82} appearing to be the most abundant dimetal compound.

Whether the metal ions are trapped inside or are outside the fullerene cage, or are incorporated into the cage structure itself, is difficult to determine because of both the small sample sizes and the variety of C_n impurities present in the samples. We have chosen to use X-ray absorption spectroscopy (XAS) to provide direct information about the environment of the Y ion in these samples. XAS is a particularly suitable technique to study this problem because it is a single ion probe, and therefore by tuning the energy to the absorption edge of interest, it is possible to determine electronic and environmental information about a specific ion in a complex matrix.

Experiments

Sample Preparation and Characterization. The metallofullerene samples were prepared in our carbon plasma generator.⁷ A 4.3-mm-diameter hole was drilled into a carbon rod of 6.3-mm thickness at a length of 38 mm. This rod was filled with a mixture of Y_2O_3 and graphite of equal volume quantities. The mixture was pressed into the tube, but no binder was used. This rod was inserted in the fullerene generator, carefully pumped down to 10^{-2} Torr, and burned under our usual experimental conditions for fullerene production.⁷ The soot obtained was collected with no special precautions to prevent air exposure. The soot was sonicated in toluene and centrifuged. The solution was decanted from the residue and dried. A mass spectrum of the material obtained by this procedure is shown in Figure 1a. The synthesis yielded the well-known distribution of all-carbon molecules, the fullerenes $C_{60}, C_{70}, C_{72}, \dots, C_{2n}$ up to very high masses (≈ 3000 amu). Other peaks are observed in the mass spectrum between the fullerene molecules, which are identified as series of YC_{2n} and Y_2C_{2n} molecules. The identified YC_{2n} molecules are YC_{60}, YC_{64} , and larger YC_{2n} entities, with $2n$ up to 100 and more. The most abundant molecules of this series are $YC_{60}, YC_{70}, YC_{76}$, and YC_{82} at $m/z = 929, 977, 1001,$ and 1073 amu, respectively. The smallest molecule observed of the Y_2C_{2n} series is Y_2C_{74} , and

* Permanent address: Institute for Surface and Interface Science, University of California, Irvine, CA 92717.

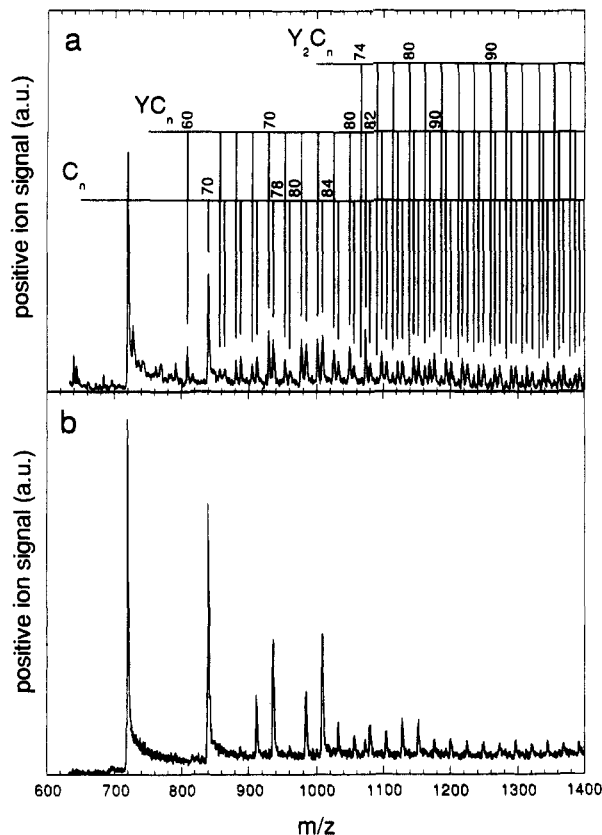


Figure 1. Time-of-flight mass spectra of positive ions, directly desorbed by pulsed 266-nm laser irradiation: (a) toluene extract of soot containing the all-carbon fullerenes C_n and metallofullerenes YC_n and Y_2C_n ; (b) toluene extract of soot containing the all-carbon fullerenes C_n and only the metallofullerenes YC_{76} and YC_{82} at $m/z = 1001$ and 1073 amu, respectively.

increased abundance in this series is found for Y_2C_{78} , Y_2C_{82} , Y_2C_{88} , and Y_2C_{94} at $m/z = 1114$, 1162 , 1234 , and 1306 amu, respectively. Performing a milder extraction at room temperature mainly dissolves YC_{82} and a little YC_{76} (less than 20%), together with the all-carbon fullerenes (Figure 1b). The other metallofullerenes remain in the residue after centrifuging and decanting the solvent. Although the total amount of YC_{82} in the sample depicted in Figure 1b is very small, it is used for X-ray absorption analysis.

X-ray Absorption Spectroscopy. Yttrium K-edge (17038 eV) X-ray absorption data were obtained on beamline X23-A2 at NSLS. Approximately 2-mg total weight of sample was used, which ultimately limited the data quality. The data on the metal fullerene samples were obtained in the electron yield and fluorescence mode using a Lytle detector, with the best detection resulting from the E-yield signal. The data for the standards were collected in the transmission mode, with a reference channel collected simultaneously. Si (311) crystals were used with 2-mm slits in order to maximize flux on sample.

Extended X-ray absorption fine structure (EXAFS) is described by scattering theory⁸⁻¹⁰ as

$$\chi(k) = \sum_j F_j(k) N_j S_j(k) \exp(-2\sigma_j^2 k^2) \exp(-2r_j/\lambda_j(k)) \times \sin(2kr_j + \phi_j(k)) (kr_j^2)^{-1}$$

where k is the scattering wavevector, and the sum is over the j coordination shells. N_j are the number of atoms in the j th coordination shell with the $F_j(k)$ backscattering amplitude. The first exponential term accounts for thermal motion and static disorder, and the second exponential represents the inelastic losses that arise during the scattering processes. $S_j(k)$ is an amplitude reduction factor representing many-body effects, and $\phi_j(k)$ is the total phase shift experienced by the photoelectron. The backscattering amplitude and phase factors are abstracted from data obtained on well-characterized standards, and the Debye-Waller

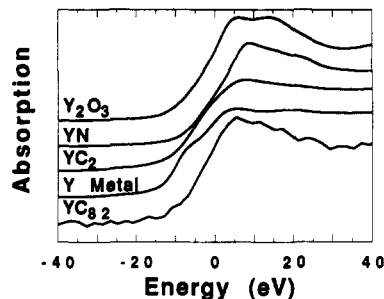


Figure 2. Near edge absorption spectra of the YC_{82} sample shown in Figure 1b, along with several standards. The edge is expected to shift to higher energy with increasing oxidation state. The edge position of YC_{82} is consistent with trivalent Y in the sample.

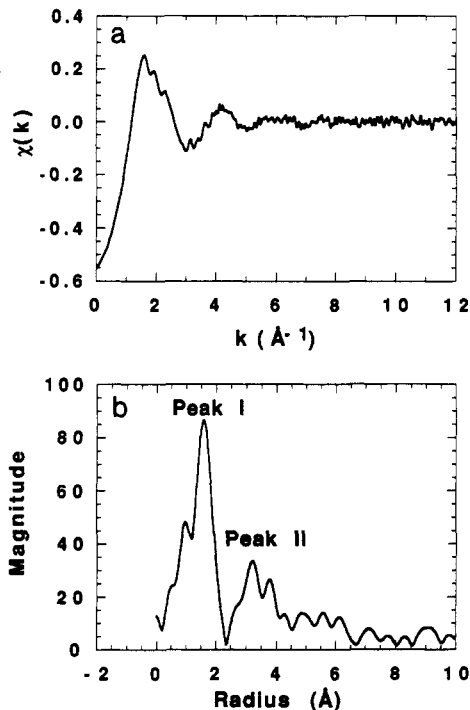


Figure 3. (a) Background subtracted EXAFS data of YC_{82} , plotted against the scattering wavevector, and (b) the Fourier transform of the data shown in (a). The two peaks in the FT are attributed to Y-C (peak I) and Y-Y (peak II) backscattering.

and disorder parameters obtained from the fitting procedures are relative to the standards. The errors reported for the fitted parameters are determined by combining errors from repeatedly fitting the data, from fitting comparable compounds, and from testing transferability on model materials.

Results

XANES. A comparison of several Y near-edge spectra is shown in Figure 2. The total, normalized step height of the electron yield spectra of the YC_{82} sample is about 0.015, reflecting both the small total sample size (about 2 mg) and the low concentration of the Y-containing phase in the sample. This step height can be compared to a normalized step height of about 1, determined from transmission mode spectra, found for samples which contain approximately 100 mg Y/cm².

The edge obtained from the YC_{82} sample occurs at a slightly higher energy than Y metal, or the other standards used here for comparison. Since the absorption edge is known to shift to higher energy with increasing charge at the central ion, the Y in our sample is shown to have a relatively low electron density, consistent with trivalent Y.

EXAFS. The background-subtracted EXAFS data, obtained from the YC_{82} sample shown in Figure 1b, are shown in Figure 3a, and the Fourier transform of these data are shown in Figure 3b. Other samples, which contain the variety of Y_xC_n species

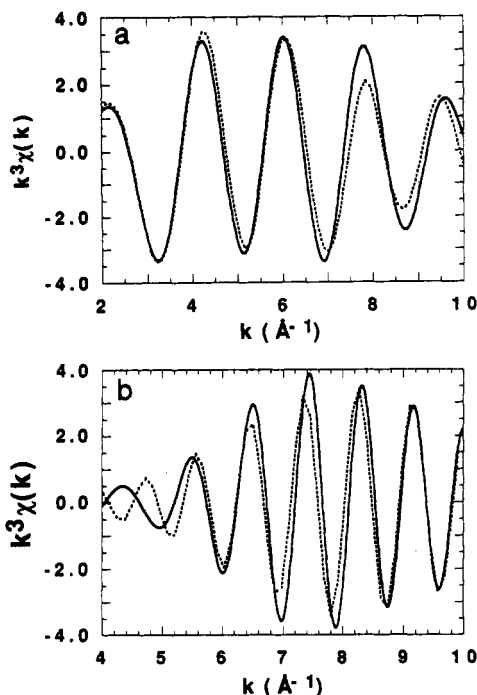


Figure 4. (a) Back-transform of peak I (solid line) and the best fit (dotted line) obtained with $N = 7 \pm 1$, $r = 2.34 \pm 0.02 \text{ \AA}$, $\sigma^2 = 0.000 \pm 0.002$, and $E_0 = -1.0 \pm 0.1$. (b) The back-transform of peak II (solid line) and the best fit (dotted line) obtained with $N = 1.5 \pm 1$, $r = 4.05 \pm 0.05 \text{ \AA}$, $\sigma^2 = 0.001 \pm 0.003$, and $E_0 = 2.7 \pm 0.3$.

depicted in Figure 1a, do not produce the well-defined peaks observed in Figure 3b but instead appear much more complicated. The only sample that produces EXAFS data simple enough to analyze is the sample that produces the mass spectrum shown in Figure 1b. This is the only sample to have predominantly one environment for the Y ion that we have studied.

The two peaks identified in Figure 3b are centered at $r' \approx 1.5 \text{ \AA}$ (peak I) and $r' \approx 3.5 \text{ \AA}$ (peak II). These peaks are analyzed separately. The back-transform of peak I is shown in Figure 4a. This peak is attributed to Y–C scattering. In order to analyze this pattern quantitatively, it is necessary to abstract the phase and amplitude functions from a standard. An Y–C compound that meets the strict requirements for a standard was not available, so YN was used instead. YN has several advantages as a standard: it is cubic (space group $Fm\bar{3}m$) with six N as Y near neighbors, all equidistant at 2.438 \AA . The use of an Y–N standard for Y–C data was indirectly checked by using YN as a standard for Y_2O_3 . Both the Y–O distances and the number of Y near neighbors refined to the known values for this material. The transferability of Y–N ($Z_N = 7$) to Y–O ($Z_O = 8$) is good evidence that YN can also well represent Y–C ($Z_C = 6$) scattering. Using YN as a standard, we obtain the one-shell fit shown in Figure 4a. The best fit to the data determines that there are 7 ± 1 equidistant near-neighbour C atoms at a distance of $2.35 \pm 0.02 \text{ \AA}$ to the Y ion.

The back-transform of peak II is shown in Figure 4b. The maximum in amplitude of the EXAFS oscillations as a function of $k \text{ (\AA}^{-1}\text{)}$ that occurs at about 7.5 \AA^{-1} is characteristic of an Y–Y backscattering function and uniquely identifies a Y as neighbor(s). Using Y–Y backscattering and phase functions obtained experimentally from YN, the data are fitted with 1–2 Y neighbors at a distance of $4.05 \pm 0.05 \text{ \AA}$. Comparing the fit to experiment (Figure 4b) shows that the fitted phase does not well match that obtained experimentally at low k . This disparity between the calculated and experimental EXAFS oscillations can be partially removed by a two-shell fit that includes both C and Y contributions. However, the details of this fit are somewhat unsatisfactory. We conclude that the disagreement shown in Figure 4b is the result of a nearly collinear arrangement of a Y–X–Y moiety that causes strong forward focusing and changes the phase from the simple phase shift of Y–Y bonding. This behavior has been previously

observed for selected shells in both NiO^{11} and YN.¹² It should be stressed that whatever the cause of the phase shift at low k , the reasonable values of N and σ^2 uniquely establish the Y–Y interaction at 4.05 \AA .

Discussion

The EXAFS data reveal an Y–C distance of $2.35 \pm 0.02 \text{ \AA}$. This distance is considerably shorter than the Y–C distances of $\approx 2.45 \text{ \AA}$ in YC_2 , the Y–N distance of 2.438 \AA in YN, and the 2.580 (3) \AA extrapolated for the π -bonded compound $Y(\eta\text{-Bu}'_3C_6H_5)_2$.¹³ The short Y–C distance indicates a strong interaction between the metal ion and the fullerene. This strong interaction is consistent with the apparent stability of our sample to reaction with moist air.

The interaction between the fullerene cage and the metal ion is further clarified by the determination of 7 ± 1 C atoms coordinated to the Y. The number of near neighbors, together with the Y–C distances, rules out the possibility that the Y ion sits at the center of the fullerene cage. This result also appears inconsistent with the suggestion that the Y ion could be incorporated into the C network that forms the cage structure,⁶ because the Y would be expected to have no more than four near-neighbor C atoms. In contrast, this result suggests that the Y ion is strongly bonded to the fullerene and is located over one of the five- or six-membered rings associated with the cage. The coordination determined here is different from that observed for osmylated C_{60} , in which the O–Os–O unit has added across a six–six ring fusion.¹⁴ The geometry determined for the Y– C_{82} suggests instead a π -bonding interaction, although our Y–C distance is considerably shorter than those observed for other Y π -bonded systems.¹³ Although π -bonding is not commonly observed for rare-earth ions, there are structures reported for $R(\eta\text{-Bu}'_3C_6H_5)_2$,^{13,15} and $R(C_6H_5)_3$,^{16,17} where $R =$ rare earth (including Sc and Y). Details of the metal–arene ring bonding are not currently understood but are discussed in general terms elsewhere.^{15,18}

The peak observed in the Fourier transformed data labeled peak II in Figure 3b arises from a Y–Y interaction at $4.05 \pm 0.05 \text{ \AA}$, considerably longer than the Y–Y distance of 3.556 \AA found in the metal or the 3.66 \AA found in the dicarbide. The relative intensities of peaks I and II in the EXAFS data are used to estimate that at least 70% of the Y contributing to peak I (attributed to Y–C scattering) is also contributing to peak II (the peak arising from Y–Y scattering). In other words, the Y–Y peak does not arise from a small impurity phase, relative to the YC_n phase, but is instead related to the major, Y-containing phase in the sample.

The determination of about seven equidistant C atom near neighbors, together with the presence of an Y–Y interaction at about 4.05 \AA , furthers the understanding of the structure of the metal–fullerene species in our sample. There are three possibilities to consider: (1) the Y ions are inside the fullerene cage, (2) one Y is inside and another is outside the cage, or (3) the metal ions are outside the cage. These possibilities are each discussed in turn.

From a geometric perspective, an Y–Y dimer would fit inside a fullerene cage. The sum of the two ring centroid–Y distances of 2.20 \AA and the Y–Y distance of 4.05 \AA is 8.45 \AA . If the C_{82} is assumed to be elliptical,¹⁹ with the Y–Y bond aligned parallel to the major ellipse axis, and if the fullerene is slightly expanded,²⁰ there may be adequate space inside the cage. However, there are several problems associated with this structural model. If the Y–Y bond is aligned along the elliptical axis of the fullerene cage, it is estimated that there should be at least 12 other C atoms at distances of about 2.5 \AA that would contribute to the EXAFS spectra. Backscattering from these other C atoms is ruled out by our data. Another problem is the charge associated with the single fullerene cage. The data presented here, as well as independent XPS⁵ and EPR⁴ data on either La or Y samples, confirm that the metal ion is trivalent. If there are two Y^{3+} ions associated inside one fullerene, then both the Coulombic repulsion between the two charges and the -6 charge associated with the cage structure would be expected to significantly destabilize the cluster. However, there is experimental evidence that both C_{60} and C_{70}

can accept six more electrons in solution.²¹ It should be noted that the Y–Y distance is too short to arise from two Y ions inside adjacent fullerene cages.

Perhaps our most significant problem with a structure in which both Y are inside the cage is the absence of any evidence of an Y_2C_n species in our mass spectral data for this EXAFS sample. Our work on other samples convinces us that we can detect Y_2C_{82} by our TOFMS experimental procedure. Furthermore, samples with multiple YC_n components, as detected by TOFMS, produce EXAFS spectra too complex for us to analyze. A structural model involving Y or an Y–Y dimer inside the fullerene cage is difficult to reconcile with the TOFMS and EXAFS data obtained from our sample.

Instead of the Y–Y inside the fullerene cage, it is possible that one Y is inside and the other outside the cage. This structure would be consistent with the TOFMS if it is assumed that the outside Y ion is only weakly bound and is easily lost in the ionization process. However, the C_n cage would still necessarily assume a –6 charge. Furthermore, the Y–Y and Y–C distances are not consistent with two Y bonding across the cage. The ring centroid–Y distance is 2.2 Å, a distance that would require the two Y to be 4.4 Å apart, but the experimentally determined Y–Y distance is only 4.05 Å. Therefore, we believe that our data are not consistent with this interpretation.

The third possibility is that both Y ions are outside the fullerene cage. We believe that this model is most consistent with our data. We propose a structure in which the two Y ions are each associated with a *different* fullerene cage and the two YC_n moieties are weakly associated, with a Y–Y distance of 4.05 Å. It is unlikely that two Y^{3+} would be directly bonded, since Coulombic repulsion would make this interaction unstable. Instead, we suggest a carbon- or oxygen-based bridge (–X–) between the two Y, to form $C_{82}Y-X-YC_{82}$ (I). We know from the analysis of peak I that the Y–X distance is about 2.35 Å, and we also know that the Y–Y distance is 4.05 Å. From these distances, we determine that the Y–X–Y angle is 150°, which is consistent with the forward focusing and subsequent complex phase shift observed in our Y–Y EXAFS. Furthermore, if the –X– bridging species could accept two electrons (one from each $C_{82}Y^-$), then our overall structure could also be used to reconcile the expectation that the cage accepts two electrons with the observation of Y^{3+} . An $(-X-)^{2-}$ could be easily understood if the –X– bridge is oxygen, the presence of which has been reported in some metallofullerene samples.^{5,6} The EXAFS results presented here cannot distinguish between oxygen and carbon atoms as near neighbors.

In order to explain the TOFMS data, it is necessary to assume that dimer I either is not stable enough to be directly observed or does not itself form ions, but instead fragments into the observed $C_{82}Y$ ions. Furthermore, the C_{82} –Y bonding would have to be strong enough to survive the ionization. The short Y–C distance observed experimentally is consistent with a strong bond, although metal–arene bonding is generally not energetically stable for C_5 and C_6 conjugated systems, which are known to be air and moisture sensitive, although they are thermally stable.¹³ However, it may be misleading to extrapolate these smaller systems to the molecules under discussion here because the much larger π -system provided by the fullerene may well afford increased stability from both electronic and steric considerations.

Whichever of these metallofullerene structures proves correct, it must necessarily be consistent with the results presented here. Our data unequivocally show that (1) Y is trivalent, (2) Y has about seven near-neighbor C atoms, and (3) there is an Y–Y interaction at a distance of 4.05 Å, which is representative of the bulk of the Y in the sample. Clearly, further experimentation is required before the structure and bonding of the metal–fullerenes are well understood.

Conclusions

The analysis of our XAS data leads us to conclude that the Y ions in our sample are trivalent and may not be inside the fullerene cage. They are strongly bonded over a five- or six-membered ring component of the cage. Our data suggest to us a model in which $C_{82}Y$ moieties couple through a bridging carbon or oxygen species to form a dimer. The existence of the molecule $C_{82}Y-X-YC_{82}$ is consistent with all of our data on this “ YC_{82} ” sample.

Acknowledgment. We thank Chuck Bouldin (NIST), G. L. Goodman, and Urs Geiser for insightful discussion. This work is supported by DOE-BES, Chemistry and Materials Sciences, all under Contract W-31-109-ENG-38.

References and Notes

- Heath, J. R.; O'Brien, S. C.; Zhang, Q.; Liu, Y.; Curl, R. F.; Kroto, H. W.; Tittel, F. K.; Smalley, R. E. *J. Am. Chem. Soc.* **1985**, *107*, 7779.
- Weiss, F. D.; Elkind, J. L.; O'Brien, S. C.; Curl, R. F.; Smalley, R. E. *J. Am. Chem. Soc.* **1988**, *110*, 4464.
- Chai, Y.; Guo, T.; Jin, C.; Haufler, R. E.; Felipe Chibante, L. P.; Fure, J.; Wang, L.; Alford, J. M.; Smalley, R. E. *J. Phys. Chem.* **1991**, *95*, 7564.
- Johnson, R. D.; deVries, M. S.; Salem, J.; Bethune, K. S.; Yannoni, C. S. *Nature* **1992**, *355*, 239.
- Weaver, J. H.; Chai, Y.; Kroll, G. H.; Jin, C.; Ohno, T. R.; Haufler, R. E.; Guo, T. R.; Alford, J. M.; Conceicao, J.; Chibante, L. P. F.; Jain, A.; Palmer, G.; Smalley, R. E. *Chem. Phys. Lett.*, submitted for publication.
- Alvarez, M. M.; Gillan, E. G.; Holczer, K.; Kaner, R. B.; Min, K. S.; Whetten, R. L. *J. Phys. Chem.* **1991**, *95*, 10561.
- Parker, D. H.; Wurz, P.; Chatterjee, K.; Lykke, K. R.; Hunt, J. E.; Pellin, M. J.; Hemminger, J. C.; Gruen, D. M.; Stock, L. M. *J. Am. Chem. Soc.* **1991**, *113*, 7499.
- Sayers, D. E.; Lytle, F. W.; Stern, E. A. *Phys. Rev. Lett.* **1971**, *27*, 1204.
- Via, G. H.; Sinfelt, J. H.; Lytle, F. W. *J. Chem. Phys.* **1979**, *71*, 690.
- Teo, B. K. In *EXAFS: Basic Principles and Data Analysis*; Springer-Verlag: New York, 1986.
- Lytle, F. W. In *Applications of Synchrotron Radiation*; Gordon and Breach: New York, 1988.
- Lytle, F. W.; Soderholm, L. Unpublished results.
- This distance is extrapolated from the Ho analogue, because Ho and Y have similar ionic radii. Data taken from: Anderson, D. M.; Cloke, F. G. N.; Cox, P. A.; Edelstein, N.; Green, J. C.; Pang, T.; Sameh, A. A.; Shalimoff, G. *J. Chem. Soc., Chem. Commun.* **1989**, 53.
- Hawkins, J. M.; Meyer, A.; Lewis, T. A.; Loren, S.; Hollander, F. J. *Science* **1991**, *252*, 312.
- Brennan, J. G.; Cloke, F. G. N.; Sameh, A. A.; Zalkin, A. *J. Chem. Soc., Chem. Commun.* **1987**, 1668.
- Wilkinson, G.; Birmingham, J. M. *J. Am. Chem. Soc.* **1954**, *76*, 6210.
- Birmingham, J. M.; Wilkinson, G. *J. Am. Chem. Soc.* **1956**, *78*, 42.
- Atwood, J. L.; Smith, K. D. *J. Am. Chem. Soc.* **1973**, *95*, 1488.
- Cotton, F. A.; Schwartz, W. *J. Am. Chem. Soc.* **1986**, *108*, 4657.
- Manolopoulos, D. E.; Fowler, P. W. *Chem. Phys. Lett.* **1991**, *187*, 1.
- Kikuchi, K.; Nakahara, N.; Wakabayashi, T.; Suzuki, S.; Shiromaru, H.; Miyake, Y.; Saito, K.; Ikemoto, I.; Kainosho, M.; Achiba, Y. *Nature* **1992**, *357*, 142.
- Cioslowski, J.; Fleischmann, E. D. *J. Chem. Phys.* **1991**, *94*, 3730.
- Xie, Q.; Perez-Cordero, E.; Echegoyen, L. *J. Am. Chem. Soc.* **1992**, *114*, 3978.